

Effect of phonons on the Josephson current density in superconductor–normal-metal–superconductor junctions with a strong-coupling normal layer

W. Lee

School of Physics and Materials, Lancaster University, Lancaster LA1 4YB, United Kingdom

(Received 8 March 1994)

We consider SNS junctions with a strong-coupling normal layer N , and calculate the Josephson critical current density J_c as a function of the electron-phonon coupling properties of the N layer. It is shown quantitatively that J_c drops quickly as the coupling strength increases and that in thick junctions with the thickness $2b \gtrsim 2\pi(\Delta_S/\hbar\omega_{\text{ph}})\xi_S$, the falling rate depends only on the coupling constant λ regardless of the spectrum of $\alpha^2F(\omega)$.

I. INTRODUCTION

The Josephson effect in a superconductor–normal-metal–superconductor (SNS) junction¹ arises from the phase-coherent quasiparticle dynamics between the two NS boundaries of the junction, rather than from “Cooper pair tunneling” as in the superconductor-insulator-superconductor junction.

Quasiparticles (holes) incident on a region where the superconducting order parameter is spatially varying have a finite probability of being Andreev reflected² as quasiholes (particles). In the N layer of an SNS junction, particles moving in the direction \hat{p} and holes moving in the $-\hat{p}$ direction are closely coupled by means of this process. Whenever they are twice Andreev reflected from the two NS boundaries of the junction, they return to their original state. However, since the magnitudes of the momenta of quasiparticle and quasihole states at the same energy ε are slightly different ($p - q \approx 2\varepsilon/v_F$), there appears a *beat* pattern in the wave function of the combined state. The density of states for the quasiparticles in the N layer, therefore, shows corresponding interference structures, such as de Gennes–Saint-James bound states³ below the lower energy gap of the two superconducting layers and the McMillan-Rowell,⁴ or the compound oscillations⁵ above the gap. In each case the *period* in the structure is $\hbar v_x^* \pi / 2b$, where $2b$ is the N -layer thickness and v_x^* is the \hat{x} (perpendicular to the NS boundaries) component of the renormalized Fermi velocity. In the presence of a phase difference $\varphi = \phi_1 - \phi_2$ between the order parameters of the two superconducting layers, a quasiparticle which is twice Andreev reflected at the two boundaries effectively picks up the phase difference φ , and the energy where the interference structure appears becomes shifted by $E_\varphi = -\hbar v_x^* \varphi / 4b$. This phase dependence of the density of states determines the Josephson current $J(\varphi)$, which is naturally dependent on the electronic transport properties of the N layer.

If N is a strong-coupling metal, phonons not only renormalize the quasiparticle properties but can also scatter electrons, destroying the interference of the phase-coherent quasiparticles. The Josephson effect is thus favored by the weaker electron-phonon coupling.

Since the quasiparticle transport in the presence of the phonon relaxation and renormalization is well understood in condensed-matter physics, the observable quantities in the strong-coupling SNS junctions, such as the temperature, or the N -layer-thickness dependence of the Josephson current, must be predictable in terms of the coupling properties. One could, for instance, tell quantitatively how *unfavorable* it is for an SNS junction to exhibit the Josephson effect if the strong-coupling properties of the materials are known. Conversely, a measurement of the Josephson effect could yield information on the electron-phonon coupling properties of an SNS system. With high-temperature superconductors,⁶ the range of possibilities of probing the N as well as the S of the SNS system seems to have become wider.

In this paper we investigate the relation of the Josephson current to the electron-phonon coupling of the N layer of an SNS junction. For this we consider an SNS system consisting of a strong-coupling normal layer with Einstein phonons, and calculate the critical Josephson current density as a function of the electron-phonon coupling properties. Several authors^{7–11} have studied the Josephson effect in SNS junctions, and calculated the Josephson current in some idealized model configuration using a variety of methods. We adopt the simplified model configuration used previously,^{7–9} and will assume the same Fermi surface parameters (the effective mass, Fermi velocity) for all three layers. The pair potential $\tilde{\Delta}$ adopts the *step approximation* and at the boundaries the matching is assumed to be perfect, which means there is no normal reflection there.

A brief description of the theoretical basis is given in Sec. II. In Sec. III we present the numerical results for the critical Josephson current density J_c , and discuss its dependence on the phonon frequency ω_{ph} and the electron-phonon coupling strength λ .

II. BASIC THEORY

From the free-energy density $F(\mathbf{R}, \varphi)$ of a superconducting system as a function of the phase difference φ , the φ dependence of the Josephson current density J is given by¹²

$$J(\mathbf{R}, \varphi) = \frac{2e}{\hbar} \partial_{\varphi} F(\mathbf{R}, \varphi), \quad (1)$$

with¹³

$$F(\mathbf{R}, \varphi) = 2kT \int d\varepsilon \ln \left[2 \cosh \frac{\varepsilon}{2kT} \right] \int d\hat{p} \rho(\hat{p}, \mathbf{R}, \varepsilon; \varphi), \quad (2)$$

where ρ is the quasiparticle density of states, which can be determined most easily from the quasiclassical Green's function \hat{g} . The Green's function $\hat{g}(\hat{p}, \mathbf{R}, \varepsilon; \varphi)$ is a 2×2 matrix in particle-hole space and is the solution of the quasiclassical equations¹⁴ (see Ref. 15 for notation)

$$[\tilde{\varepsilon} \hat{\tau}_3 - \hat{\Delta}, \hat{g}] + i \mathbf{v}_F \cdot \nabla \hat{g} = 0, \quad (3)$$

$$\hat{g}^2 = -\pi^2, \quad (4)$$

with appropriate boundary conditions.¹⁶ The self-energy $\hat{\Delta}$ is expressed in the *real gauge*¹⁷ by

$$\hat{\Delta} = \begin{pmatrix} 0 & \tilde{\Delta} e^{i\phi} \\ -\tilde{\Delta} e^{-i\phi} & 0 \end{pmatrix}, \quad (5)$$

where the complex order parameter $\tilde{\Delta}$, together with the renormalized energy $\tilde{\varepsilon}$, is the solution of Eliashberg's gap equations.¹⁸ In the general case the gap equations must be solved self-consistently with Eq. (3), which gives the spatial dependence of the functions, $\tilde{\Delta}, \tilde{\varepsilon}$. In the step approximation, which is good in thick junctions, $\tilde{\Delta}$ and $\tilde{\varepsilon}$ are stepwise constant in space. In the normal state, $\tilde{\Delta}$ is zero and $\tilde{\varepsilon}$ reduces to the following analytical expression:¹⁹

$$\tilde{\varepsilon}_N = \varepsilon \pm \int d\omega \alpha^2 F(\omega) \left\{ i\pi \coth \frac{\omega}{2kT} - \psi \left[\frac{1}{2} - i \frac{\varepsilon - \omega}{2\pi kT} \right] + \psi \left[\frac{1}{2} - i \frac{\varepsilon + \omega}{2\pi kT} \right] \right\}, \quad (6)$$

where $\alpha^2 F(\omega)$ is the electron-phonon coupling function and ψ is the complex digamma function. In the weak-coupling limit, $\tilde{\Delta}$ reduces to the energy gap Δ and $\tilde{\varepsilon}$ becomes ε , the quasiparticle energy.

For clarity, we place the *NS* boundaries at $x = \pm b$. The boundaries are infinite in the yz plane, and the system is invariant under translation in the \hat{y}, \hat{z} directions and under rotation around the \hat{x} axis. In the step approximation, the solution of the quasiclassical equations in each layer can readily be expressed in terms of the following three trivial solutions:

$$\hat{g}_1 = -\frac{\pi}{\tilde{\Omega}} \begin{pmatrix} \tilde{\varepsilon} & -\tilde{\Delta} e^{i\phi} \\ \tilde{\Delta} e^{-i\phi} & -\tilde{\varepsilon} \end{pmatrix}, \quad (7)$$

$$\hat{g}_2 = -\frac{\pi}{\tilde{\Omega}} \begin{pmatrix} \tilde{\Delta} & -(\tilde{\varepsilon} \mp i\tilde{\Omega}) e^{i\phi} \\ (\tilde{\varepsilon} \pm i\tilde{\Omega}) e^{-i\phi} & -\tilde{\Delta} \end{pmatrix} \exp \left[\frac{2\tilde{\Omega}x}{v_x} \right], \quad (8)$$

$$\hat{g}_3 = -\frac{\pi}{\tilde{\Omega}} \begin{pmatrix} \tilde{\Delta} & -(\tilde{\varepsilon} \pm i\tilde{\Omega}) e^{i\phi} \\ (\tilde{\varepsilon} \mp i\tilde{\Omega}) e^{-i\phi} & -\tilde{\Delta} \end{pmatrix} \exp \left[-\frac{2\tilde{\Omega}x}{v_x} \right], \quad (9)$$

where $\tilde{\Omega} = \sqrt{\tilde{\Delta}^2 - \tilde{\varepsilon}^2}$, with the branch cut along the negative ε axis, and $v_x = v_F \hat{p} \cdot \hat{x}$. The \pm sign in Eqs. (8) and (9) comes from $\mathbf{v}_F \cdot \nabla = \pm v_x \partial x$, where we take advantage of the spatial symmetry of the configuration, namely, the translational invariance of the system in the \hat{y} and \hat{z} directions. The first solution \hat{g}_1 is the *bulk solution* which exactly describes the superconducting state of the isolated bulk material. The second and third basic solutions are the so-called *Tomasch solutions*, which *oscillate* with the Tomasch wavelength.²⁰ This type of solution appears whenever a system is in contact with another superconductor with different order parameter and incorporates the transfer of the particle-hole coherence from one side to the other.

In the present *ideal* model, where we assume the same Fermi velocity and the same effective mass for all layers and no boundary potential at the interfaces, the rather involved boundary conditions for the quasiclassical Green's functions reduce to a simple matching condition, namely, the continuity of the \hat{g} 's through the interface. Applying this condition to the two *NS* interfaces, we obtain the following solution for the $\hat{\tau}_3$ component of \hat{g} , at $x=0$ in the normal layer:

$$g(\hat{p}, 0, \varepsilon; \varphi) = \pi \frac{\tilde{\varepsilon}_S \cos \left[\frac{2\tilde{\varepsilon}_N b}{v_x} + \frac{\varphi}{2} \right] + \tilde{\Omega}_S \sin \left[\frac{2\tilde{\varepsilon}_N b}{v_x} + \frac{\varphi}{2} \right]}{\tilde{\varepsilon}_S \sin \left[\frac{2\tilde{\varepsilon}_N b}{v_x} + \frac{\varphi}{2} \right] - \tilde{\Omega}_S \cos \left[\frac{2\tilde{\varepsilon}_N b}{v_x} + \frac{\varphi}{2} \right]}. \quad (10)$$

The \hat{p} -resolved density of states is then given by

$$\rho(\hat{p}, 0, \varepsilon; \varphi) = -\frac{1}{\pi} \text{Im} g(\hat{p}, 0, \varepsilon; \varphi). \quad (11)$$

III. RESULTS AND DISCUSSION

In this section we evaluate the maximum Josephson current density J_c and its dependence on the electron-

phonon coupling of the *N* layer. The two *S* layers are assumed to be in the weak-coupling limit with the same energy gap Δ . In this case $\tilde{\varepsilon}_S$ and $\tilde{\Omega}_S$ in Eq. (10) reduce to ε and $\sqrt{\Delta^2 - \varepsilon^2}$, respectively. For the coupling function we assume the Einstein spectrum

$$\alpha^2 F(\omega) = \lambda \frac{\omega_{\text{ph}}}{2} \delta(\omega - \omega_{\text{ph}}), \quad (12)$$

where ω_{ph} is the single-mode phonon frequency and λ is the electron-phonon coupling constant. While the actual $\alpha^2 F(\omega)$ of a realistic system is usually a broad spectrum, Eq. (12) is useful in understanding the underlying physics of electron-phonon coupling.

As a preliminary result, $\tilde{\epsilon}_N(\epsilon)$ and $\rho(\epsilon, \phi)$ at various temperatures are shown in Figs. 1 and 2 for a choice of material parameters. The real part of $\tilde{\epsilon}_N(\epsilon)/\epsilon$ measures the effective renormalization of the quasiparticle properties. At $\epsilon=0$, it is equal to $1+\lambda$, which is the static renormalization factor. As ϵ increases to $\hbar\omega_{\text{ph}}$, the effective renormalization factor increases. It peaks at $\epsilon=\hbar\omega_{\text{ph}}$ and then drops sharply and eventually becomes unity at higher frequencies. At the same time a finite imaginary part appears at quasiparticle energies above $\hbar\omega_{\text{ph}}$, which measures the relaxation rate of quasiparticles by phonon emission and is proportional to the coupling strength λ . Correspondingly, the resonance structures in the density of states, de Gennes–Saint-James bound states and the McMillan-Rowell oscillation, deviate from the weak-coupling feature. The energy-dependent renormalization factor, which effectively makes the quasiparticle velocity v_F^* dependent on energy, gives rise to a change in the position of the bound states or the period of the oscillation below the phonon energy $\hbar\omega_{\text{ph}}$. The phonon relaxation, the imaginary part of $\tilde{\epsilon}(\epsilon)$, very strongly suppresses the resonance structure above $\epsilon=\hbar\omega_{\text{ph}}$.

These features of the electron-phonon coupling result in a reduction of the Josephson current density. Figure 3(a) shows the Josephson current density J as a function of the phase difference φ in the presence of strong coupling strengths. At $T=0$, in both the weak- and the strong-coupling cases, $J(\varphi)$ is a sawtooth function linearly increasing from $-J_c$ to J_c over each interval of φ from $(2n-1)\pi$ to $(2n+1)\pi$ [8,9]. At very low temperatures, as the $kT=0.001\Delta_S$ curves in Fig. 3 show, $J(\varphi)$ is near this limit. In the strong-coupling case, the magnitude of $J(\varphi)$ is reduced from the weak-coupling values according to the coupling strength λ . At higher temperatures, as

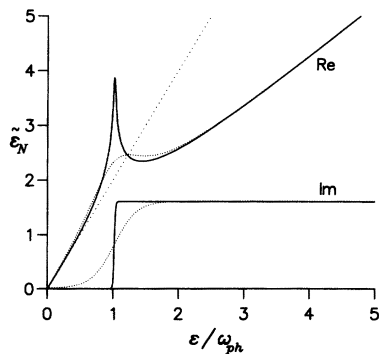


FIG. 1. Real and imaginary parts of the renormalized energy $\tilde{\epsilon}_N(\epsilon)$ for $\alpha^2 F(\omega)$ of an Einstein phonon, at temperatures $kT=0.01$ (solid line) and $0.15\hbar\omega_{\text{ph}}$ (dotted line). $\hbar\omega_{\text{ph}}$ is the phonon frequency and the coupling strength is $\lambda=1$. The slope at $\epsilon\approx 0$ of the real part of $\tilde{\epsilon}_N$ at $T=0$ (dotted straight line) is the static renormalization factor $1+\lambda$.

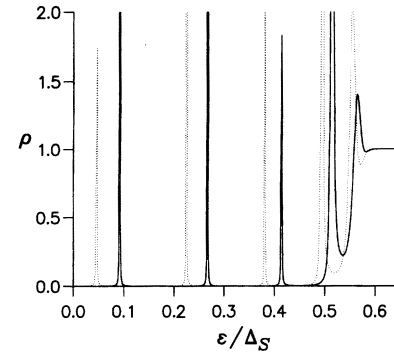


FIG. 2. The density of states $\rho(\hat{p}, 0, \epsilon; \varphi)$ for the phase differences $\varphi=0$ (solid line) and $\pi/2$ (dotted line), at $kT=0.015\Delta_S$. The momentum direction \hat{p} is such that $v_x^*=0.5v_F^*$, and the N -layer thickness is $2b=33\xi_S$, where $\xi_S=v_{FS}/2\Delta_S$. $\hbar\omega_{\text{ph}}=0.6\Delta_S$ and $\lambda=1$. The resonance energy points move down as $\hbar v_x^* \varphi/4b$ with the phase difference φ .

the thermal energy kT exceeds the bound-state level separation at smaller angle ($\hat{p}\cdot\hat{x}\rightarrow 1$), $J(\varphi)$ becomes effectively averaged within the “thermal width” kT and approaches the sinusoidal form with increasing temperature. Additionally, the amplitude falls with increasing T . In the weak-coupling case this gives a universal tempera-

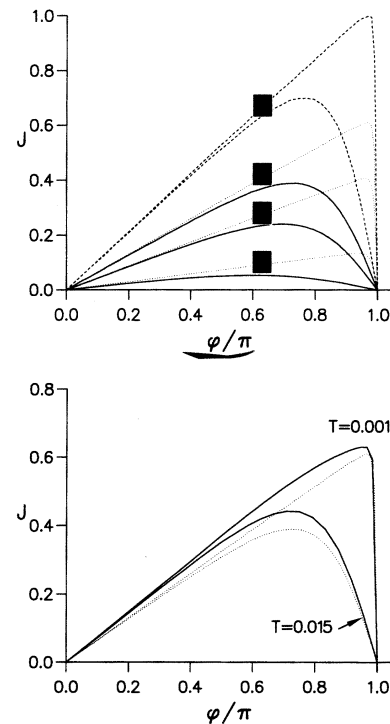


FIG. 3. (a) $J(\varphi)$ for $\hbar\omega_{\text{ph}}=0.6\Delta_S$ and various coupling strengths $\lambda=2, 0.67$, and 0.33 (the pair of curves a, b , and c , respectively) at $kT=0.001$ (solid lines) and $0.015\Delta_S$ (dotted lines). $2b=33\xi_S$. The uppermost pair of the lines (w) are the weak-coupling curves of the same configuration. (b) The ω_{ph} dependence of $J(\varphi)$ for the same configuration for $\lambda=0.33$. $\hbar\omega_{\text{ph}}=0.1$ (solid) and $0.6\Delta_S$ (dotted lines) at different temperatures $kT=0.001$ and $0.015\Delta_S$.

ture dependence of the critical current for a given sample geometry. In the strong-coupling case, the density of states itself is dependent on temperature according to the temperature-dependent quasiparticle renormalization. This results, for stronger coupling, in a more rapid decrease of the Josephson current with temperature. This feature of Fig. 3(a), shown for $\hbar\omega_{\text{ph}}=0.6\Delta_S$, does not change very much with $\hbar\omega_{\text{ph}}$. The ω_{ph} dependence (for constant λ) is negligible except at very small values of $\hbar\omega_{\text{ph}}$, where, as Fig. 3(b) shows, it results in a higher critical current density J_c .

In Figs. 4–6 we plot, as a function of various parameters, the critical Josephson current density J_c , which is the maximum value of $J(\varphi)$ normalized by the weak-coupling value of the same configuration at $T=0$. Figure 4 shows $J_c(\lambda)$ for several frequency values of the Einstein spectrum, at different temperatures. $J_c(\lambda)$ is a rapidly decreasing function of λ from the weak-coupling values at $\lambda=0$. At higher temperatures, $J_c(\lambda)$ decreases more rapidly with λ , as the inelastic electron-phonon scattering rate increases with T and λ . However, the critical current J_c is almost independent of ω_{ph} , as already shown in $J(\varphi)$, except at very low frequencies (see the $\hbar\omega_{\text{ph}}=0.1\Delta_S$ curves in the Figure), where the quasiparticle relaxation effectively cuts off the higher-energy contribution to the current [Eq. (1)]. Over the whole frequency range above this small value, the effect of the phonon on the Josephson current is well described by a single parameter, namely, the coupling constant

$$\lambda = 2 \int d\omega \frac{\alpha^2 F(\omega)}{\omega}. \quad (13)$$

The ω_{ph} dependence of J_c of constant λ is shown in Fig. 5. The frequency above which J_c has only weak ω_{ph} dependence (the “thick regime”) varies with temperature. At the low temperatures considered in the figure, it is comparable to $\omega_0 \sim \pi v_F^*/2b$, the bound-state level separation at zero angle. In a “thick” junction with $2b \sim 30\xi_S$,

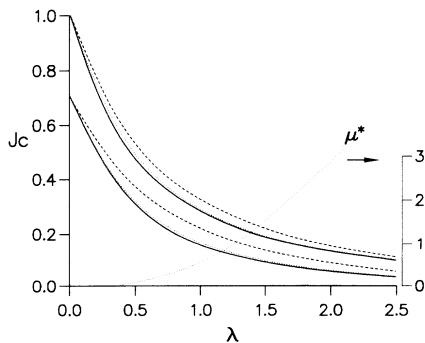


FIG. 4. $J_c(\lambda)$ for $\hbar\omega_{\text{ph}}=0.6$ (solid), 0.3 (dotted), and $0.1\Delta_S$ (dashed lines) at temperatures $kT=0.001$ (upper three) and $0.015\Delta_S$ (lower three curves). $2b=33\xi_S$. J_c is normalized by the weak-coupling value at $T=0$. The dotted line μ^* shows, as function of λ , the magnitude of the Coulomb pseudopotential needed to keep the layer N in the normal state at $kT=0.015\Delta_S$ for $\hbar\omega_{\text{ph}}=0.6\Delta_S$.

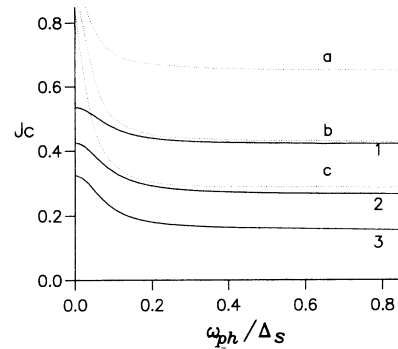


FIG. 5. $J_c(\omega_{\text{ph}})$ for $\lambda=0.3, 0.6$, and 1 , at temperatures $kT=0.001$ (the dotted curves a, b , and c) and $0.015\Delta_S$ (solid curves 1, 2, and 3). $2b=33\xi_S$. J_c is normalized by the weak-coupling value at $T=0$.

the frequency is about $\omega_0 \sim \pi\Delta_S/15$, that is, less than 1 meV for a junction with conventional superconductors. With high-temperature superconductors, where $\Delta_S \sim 20$ meV, this can be as high as ~ 5 meV. Figure 6 shows the temperature dependence of J_c . The critical Josephson current density drops quickly with temperature, and more rapidly with stronger electron-phonon coupling. In the thick regime, since J_c is independent of the spectral shape of the coupling function $\alpha^2 F(\omega)$, $J_c(T)$ gives a direct measure of the coupling constant λ . The critical current falls very rapidly also with the N -layer thickness $2b$ (Fig. 7). As the bound-state level separation becomes smaller with increasing thickness, the thick regime extends to the lower-frequency region and the decrease of J_c with temperature becomes even faster with larger $2b$. However the qualitative features shown in the previous figures remain the same.

Since T_{cN} (Ref. 21) increases with λ , for a strongly coupling N layer we need a finite repulsive Coulomb pseudopotential μ^* to keep the N layer in the normal state, if Δ_N is not otherwise suppressed. The dotted line μ^* in Fig. 4 shows, for example, the magnitude of the potential needed to ensure that $\Delta_N=0$, obtained by solving the

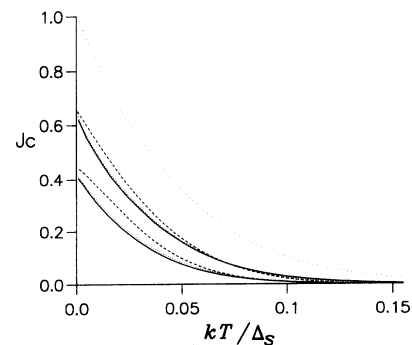


FIG. 6. $J_c(T)$ for $\lambda=0.67$ (lower three) and 0.33 (middle three), and $\hbar\omega_{\text{ph}}=0.1$ (dashed), 0.3 (dotted), and $0.6\Delta_S$ (solid lines). $2b=33\xi_S$. The additional dotted line is the weak-coupling curve. J_c is normalized by the weak-coupling value at $T=0$.

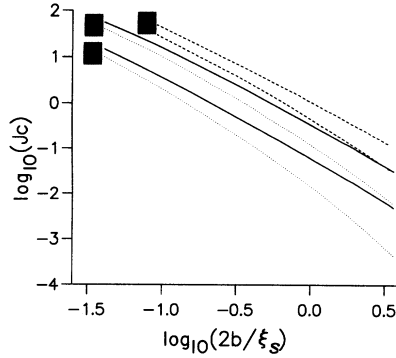


FIG. 7. $J_c(2b)$ for $\hbar\omega_{\text{ph}}=0.6\Delta_S$ and coupling constants $\lambda=1$ (pair of curves *a*) and 0.33 (pair of curves *b*) at temperatures $kT=0.001$ (solid) and $0.015\Delta_S$ (dotted lines). The pair of dashed curves (*w*) are the corresponding weak-coupling curves at $kT=0.001$ (upper) and $0.015\Delta_S$ (lower line). J_c is normalized by the weak-coupling value of $J_c(2b=33\xi_S)$ and $T=0$.

Eliashberg's equations with the parameters given in the figure. The values indicate in this case that the observable range of $J_c(\lambda)$ is for $\lambda \lesssim 1$ with reasonable values of $\mu^* \lesssim 0.5$.

In conclusion, we have numerically evaluated the effect of N -layer phonons on the Josephson current density in SNS junctions. The strong electron-phonon coupling suppresses the critical Josephson current density J_c . The dependence of J_c on the phonon frequency is negligible except for the case of couplings to a very soft phonon mode, $\omega_{\text{ph}} \lesssim \pi v_F^*/2b$. In thick junctions where the thickness is $2b \gtrsim 2\pi(\Delta_S/\hbar\omega_{\text{ph}})\xi_S$, the effect of the electron-phonon coupling on the J_c is governed by the coupling constant λ alone, regardless of the spectral shape of the coupling function $a^2F(\omega)$. Thus, in the thick regime the temperature dependence of J_c directly measures the coupling constant λ . The electron-phonon coupling of the two superconducting S layers, on the other hand, does not contribute to the quasiparticle damping in the N layer but gives rise to a phase shift in the interference pattern of $\rho(\varepsilon)$.²² The influence of this phase shift on the Josephson current is discussed elsewhere.²³

ACKNOWLEDGMENT

This work was supported by the Science and Engineering Research Council of the United Kingdom.

¹K. K. Likharev, Rev. Mod. Phys. **51**, 101 (1979).

²A. F. Andreev, Sov. Phys. JETP **19**, 1228 (1964).

³P. G. de Gennes and D. Saint-James, Phys. Lett. **4**, 151 (1963).

⁴J. M. Rowell and W. L. McMillan, Phys. Rev. Lett. **16**, 453 (1966).

⁵E. L. Wolf and G. B. Arnold, Phys. Rep. **91**, 31 (1982).

⁶D. A. Wollman, D. J. van Harlingen, W. C. Lee, D. M. Ginsberg, and A. J. Leggett, Phys. Rev. Lett. **71**, 2134 (1993).

⁷I. O. Kulik, Sov. Phys. JETP **30**, 944 (1970).

⁸C. Ishii, Prog. Theor. Phys. **44**, 1525 (1970).

⁹J. Bardeen and J. L. Johnson, Phys. Rev. B **5**, 72 (1972).

¹⁰R. Kümmel, U. Günsenheimer, and R. Nicolsky, Phys. Rev. B **42**, 3992 (1990).

¹¹W. Lee, Physica B **194-196**, 1715 (1994).

¹²B. D. Josephson, in *Superconductivity*, edited by R. D. Parks (Marcel Dekker, NY, 1969), Vol. 1, p. 423.

¹³G. Eilenberger, Z. Phys. **182**, 427 (1965).

¹⁴G. Eilenberger, Z. Phys. **214**, 195 (1968); A. I. Larkin and Yu. N. Ovchinnikov, Sov. Phys. JETP **28**, 1200 (1969).

¹⁵J. W. Serene and D. Rainer, Phys. Rep. **101**, 221 (1983).

¹⁶A. V. Zeitsev, Sov. Phys. JETP **59**, 1015 (1984); G. Kieselmann, Phys. Rev. B **35**, 6762 (1987); L. J. Buchholtz and D. Rainer, Z. Phys. B **35**, 151 (1979).

¹⁷S. V. Vonsovsky, Yu. A. Izyumov, and E. Z. Kurmaev, *Superconductivity of Transition Metals* (Springer Verlag, Berlin, 1982).

¹⁸G. M. Eliashberg, Sov. Phys. JETP **11**, 696 (1960).

¹⁹W. Lee, D. Rainer, and W. Zimmermann, Physica C **159**, 535 (1989).

²⁰J. Herath, J. Kurkijärvi, and D. Rainer, Czech. J. Phys. B **40**, 1156 (1990).

²¹D. Rainer, in *Progress in Low Temperature Physics*, edited by D. F. Brewer (Elsevier, Amsterdam, 1986), Vol. X, p. 371; P. B. Allen and B. Mitrović, in *Solid State Physics*, edited by F. Seitz, D. Turnbull, and H. Ehrenreich (Academic, New York, 1982), Vol. 37, p. 1.

²²W. Lee, J. Supercond. **7**, 613 (1994).

²³W. Lee (unpublished).

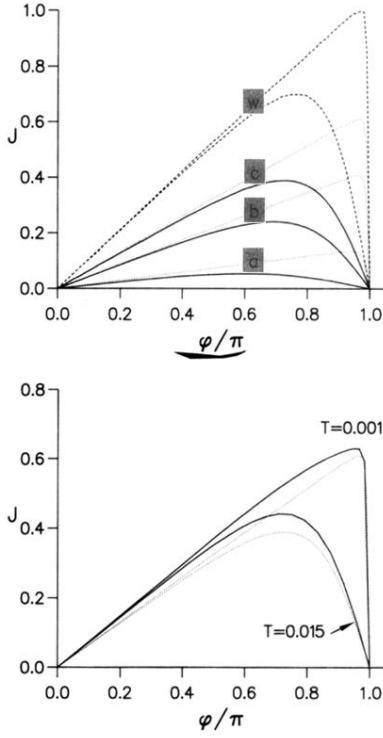


FIG. 3. (a) $J(\varphi)$ for $\hbar\omega_{ph}=0.6\Delta_S$ and various coupling strengths $\lambda=2, 0.67$, and 0.33 (the pair of curves a, b , and c , respectively) at $kT=0.001$ (solid lines) and $0.015\Delta_S$ (dotted lines). $2b=33\xi_S$. The uppermost pair of the lines (w) are the weak-coupling curves of the same configuration. (b) The ω_{ph} dependence of $J(\varphi)$ for the same configuration for $\lambda=0.33$. $\hbar\omega_{ph}=0.1$ (solid) and $0.6\Delta_S$ (dotted lines) at different temperatures $kT=0.001$ and $0.015\Delta_S$.

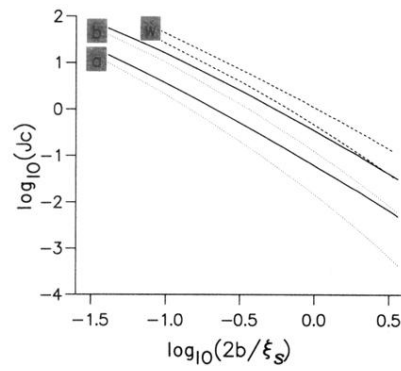


FIG. 7. $J_c(2b)$ for $\hbar\omega_{\text{ph}}=0.6\Delta_S$ and coupling constants $\lambda=1$ (pair of curves *a*) and 0.33 (pair of curves *b*) at temperatures $kT=0.001$ (solid) and $0.015\Delta_S$ (dotted lines). The pair of dashed curves (*w*) are the corresponding weak-coupling curves at $kT=0.001$ (upper) and $0.015\Delta_S$ (lower line). J_c is normalized by the weak-coupling value of $J_c(2b = 33\xi_S)$ and $T=0$.